

On the nature of Nova 1670 (CK Vulpeculae): a merger of a red giant with a helium white dwarf

Romuald Tylenda¹, Tomek Kamiński¹, and Radek Smolec²

¹ Nicolaus Copernicus Astronomical Center, Polish Academy of Sciences, Rabiańska 8, 87-100 Toruń, Poland, e-mail: tylenda@ncac.torun.pl, tomkam@ncac.torun.pl

² Nicolaus Copernicus Astronomical Center, Polish Academy of Sciences, Bartycka 18, 00-716 Warszawa, Poland, e-mail: smolec@camk.edu.pl

Received; accepted

ABSTRACT

Context. Nova 1670 is a historical transient bearing strong similarities to a recently-recognized type of stellar eruptions known as red novae, which are thought to be powered by stellar mergers. The remnant of the transient, CK Vul, is observable today mainly through cool circumstellar gas and dust, and recombining plasma, but we have no direct view on the stellar object.

Aims. Within the merger hypothesis, we aim to infer the most likely makeup of the progenitor system that resulted in Nova 1670.

Methods. We collect and summarize the literature data on the physical properties of the outburst and the remnant (including their energetics), and on the chemical composition of the circumstellar material (including elemental and isotopic abundances) which resulted from optical and submillimeter observations of the circumstellar gas of CK Vul. We perform simple simulations to analyze the form and level of mixing of material associated with the merger. Products of nuclear burning are identified, among them ashes of hydrogen burning in the CNO cycles and the MgAl chain, as well as of partial helium burning.

Results. Based primarily on the luminosity and chemical composition of the remnant, we find that the progenitor primary had to be an evolutionarily advanced red-giant branch star of a mass of 1–2 M_{\odot} . The secondary was either a very similar giant, or, more likely, a helium white dwarf. While the eruption event was mainly powered by accretion, we estimate that about 12% of total energy might have come from helium burning activated during the merger. The coalescence of a first-ascent giant with a helium white dwarf created a star with a rather unique internal structure and composition, which resemble these of early R-type carbon stars.

Conclusions. Nova 1670 was the result of a merger between a helium white dwarf and a first-ascent red giant and is likely now evolving to become an early R-type carbon star.

Key words. stars: individual: CK Vul - stars: individual: Nova 1670 - stars: activity - stars: winds, outflows - stars: variables: other

1. Introduction

On 20 June 1670, Anhelme Voituret (Dom Anhelme), a Carthusian monk in Dijon (France), spotted a new star of ~ 3 mag in the constellation of Cygnus. A month later, the star was independently found by Johannes Hevelius in Gdańsk (Poland). Since then the object was gradually fading and, in October, it became invisible to the naked eye. In March 1671, the star reappeared and on 30 April attained its maximum brightness of ~ 2.6 mag. Subsequent fading lasted till the end of August, when the star again became invisible. Next year, in March–May 1672, the object was observable for a third time, but now as a much fainter star of ~ 5.4 mag. A detailed description of historical data on Nova 1670 can be found in Shara et al. (1985). In the modern astronomy, Nova 1670 is known as CK Vulpeculae¹.

Numerous attempts to find a remnant of Nova 1670, which go back to the seventeenth century (for references, see Shara et al. 1985), failed to detect any stellar-like object. Shara et al. (1985) claimed to see a very faint star at the expected position, but later observations did not confirm that (Naylor et al. 1992). All what was found in the optical was a faint nebulosity emitting mainly in the [NII] and H α lines (e.g. Shara et al. 1985; Hajduk et al. 2007), shown in Fig. 1.

¹ The constellation of Vulpecula was introduced by J. Hevelius a few years after the discovery of Nova 1670.

Until the end of the twentieth century, Nova 1670 was primarily considered as a classical nova, that is, an event resulting from a thermonuclear runaway on the surface of a white dwarf (WD) accreting H-rich matter in a binary system. This false identification of Nova 1670 was claimed despite the obvious problem that the light curve clearly did not resemble these of classical novae (including slow novae). Indeed, it had two well-defined peaks separated by almost a year and followed by a much dimmer peak next year (see Fig. 2 in Shara et al. 1985). Moreover, it appeared that CK Vul was relatively bright in the far-infrared (IR) and submillimeter range (Evans et al. 2002). With the absence of any stellar emission in the optical, this implies that the remnant of Nova 1670 is embedded in a thick, dusty envelope. Nothing of the sort has been observed in any of the historical classical novae (cf. Kamiński et al. 2022).

These facts have prompted some authors to postulate that Nova 1670 was the case of a (very) late He-shell flash in a post asymptotic giant branch (post-AGB) star, similar to V605 Aql or V4334 Sgr (Harrison 1996; Evans et al. 2002). There are, however, fundamental problems with the luminosity evolution in such a scenario. Namely, Nova 1670 had $\sim 10^7 L_{\odot}$ at maximum, while CK Vul has only a few tens solar units at present (see Sect. 2.4), that is, the object faded by more than five orders of magnitude during ~ 340 years. This is to be compared to a typical luminosity of a post-AGB star, which is of the order of

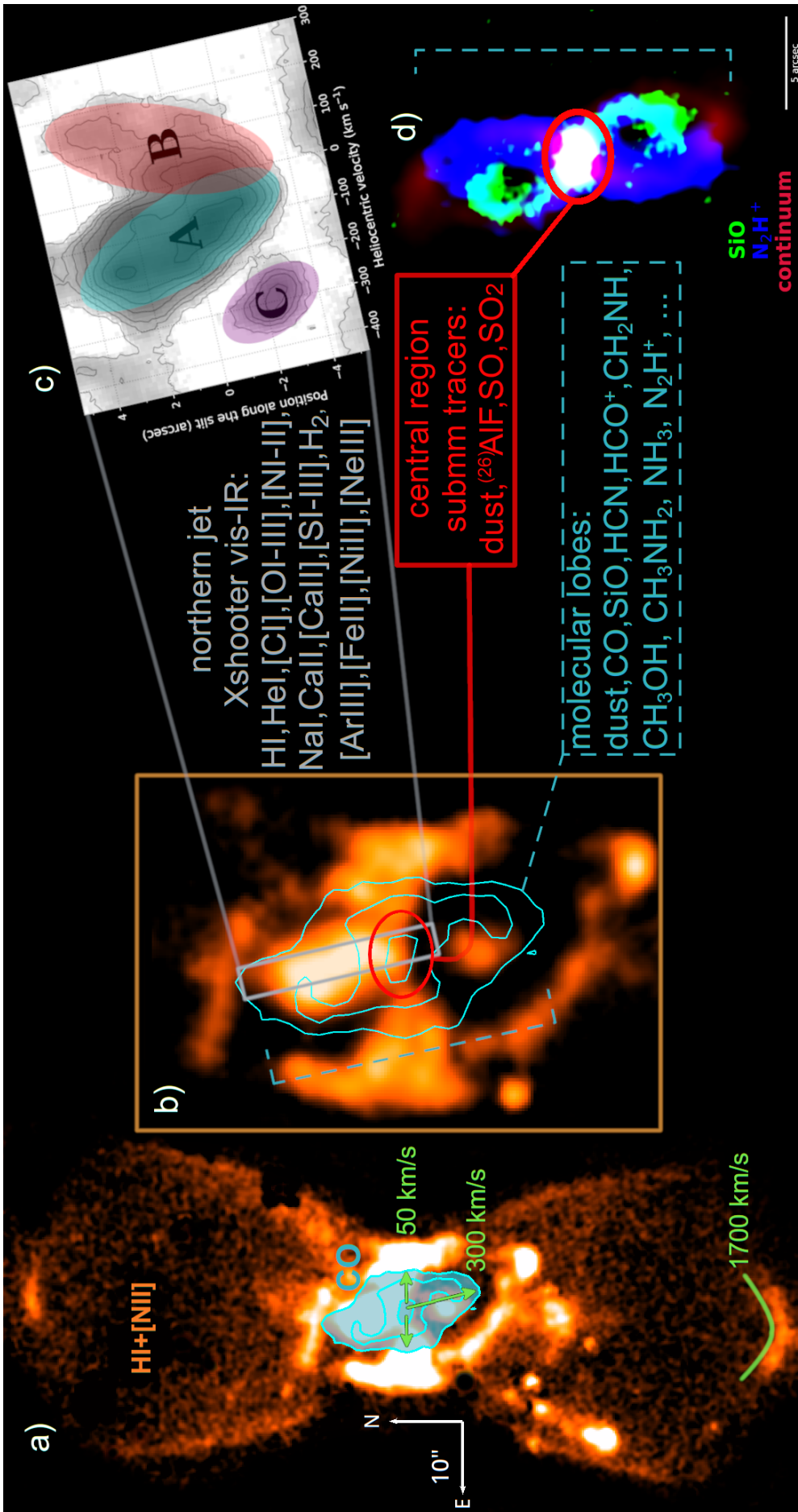


Fig. 1. Components of the nebulae surrounding CK Vul. **a)** Optical hourglass nebula (orange and white) seen in the combined emission of H α and [NII] lines (from Hajduk et al. 2013). Millimeter-wave emission of CO 1–0 is overlaid in cyan (from Kamiński et al. 2020). Green markers and labels show characteristic velocities of these components. **b)** Zoomed-in central portion of the components shown in a). The structure of the optical nebula is seen more clearly. The red ellipse indicates the central region where many O-bearing molecules and strong dust emission are observed. The gray rectangle shows the region within the northern optical “jet” observed spectrally in the optical–near-infrared with Xshooter at a very high sensitivity (Tylenda et al. 2019). **c)** The inset shows dispersed emission of a spectral line within the northern jet and illustrates that the emission is composed of at least three distinct morpho-kinematical components. **d)** Combined emission of SiO (green), N₂H⁺ (blue), and mm-wave continuum define the molecular nebula (from Kamiński et al. 2020). The central region, bright in dust emission, is marked with a red ellipse.

$10^4 L_{\odot}$ and does not change significantly during the He-shell flash. Even if one neglects the absolute values (e.g., arguing that the distance to CK Vul is uncertain), within the post-AGB hypothesis the luminosity drop would mean that CK Vul is below $0.1 L_{\odot}$. First, the evolution of a post-AGB star to that luminosity would take a million years or more (e.g. Blöcker 1995; Miller Bertolami 2016), orders of magnitude longer than the age of CK Vul. Second, it would imply a distance of a few tens of pc, well below any distance estimate existing in literature. Nova 1670 could not result from a late He-shell flash in a post-AGB star.

The eruption of V838 Mon in 2002 (Munari et al. 2002; Kimeswenger et al. 2002; Crause et al. 2003) was one of the most exciting and intriguing events in stellar astrophysics of a few past decades. Astrophysicists started to realize that there exists a class of stellar outbursts that does not fit to any of known and understood mechanisms of stellar eruptions. The eruptions of this new type, named red novae or red transients, show a particular spectral evolution: in the course of the outburst the spectrum evolves towards progressively later types, down to a late M-type in the decline. Following the idea outlined in Soker & Tylenda (2003), Tylenda & Soker (2006) showed that the principal characteristics of red novae can be understood in terms of a hypothesis that these eruptions result from stellar mergers. Soon after, the hypothesis received strong observational support. It was mainly presented in Tylenda et al. (2011), who showed that V1309 Sco was a contact binary just before its red nova outburst in 2008.

Following the idea of Soker & Tylenda (2003), Kato (2003) suggested that Nova 1670 might have also resulted from a stellar merger. The author drew attention to similarities between the light curve of Nova 1670 and that of V838 Mon. Although the light curves of both objects display three brightness peaks, the timescale of the outburst of Nova 1670 is an order of magnitude longer than that of V838 Mon and, in fact, of any other red nova known at that time. This raised certain objections against the Kato's interpretation of Nova 1670. However, Tylenda et al. (2013) discovered a red nova in the archives of the OGLE project, OGLE-2002-BLG360, whose light curve showed multiple peaks on a timescale similar to that of Nova 1670. This revived the interest in Nova 1670 as a probable red nova.

Following the finding of Tylenda et al. (2013), an extensive study of CK Vul in the (sub)millimeter range was undertaken (Kamiński et al. 2015, 2017, 2018, 2020). The project provided us with the data strongly supporting the hypothesis of the red-nova nature of Nova 1670. In the present paper, we summarize the results of this project and of other studies. We then show that they can be consistently interpreted in terms of a merger of a red-giant-branch (RGB) star with a helium white dwarf (HeWD).

2. Observational results

2.1. The remnant

At present, the remnant of Nova 1670 (CK Vul) is observed at optical and (sub)millimeter (submm) wavelengths as a bipolar nebula. Figure 1 summarizes its components. In the optical, a faint emission-line nebula of an hourglass shape is visible, mainly in $H\alpha$ and [N II] lines (Shara et al. 1985; Hajduk et al. 2007). The bipolar lobes extend up to $\sim 36''$ from the hourglass center. Detailed optical spectroscopy of the brightest clump close to the center of the nebula revealed a rich, low-excitation nebular spectrum (Tylenda et al. 2019). No central stellar-like object has been identified so far. Evidently, it is hidden in a dense, dusty central region of the remnant (see below).

In the submm range, the object displays a very rich spectrum of molecular emission lines (Kamiński et al. 2015, 2017). The emission region shows again a bipolar structure, although it is more compact than the optical nebula. The submillimeter emission of molecules and dust extend only up to $\sim 8''$ from the center (Kamiński et al. 2020). Also, the axis of symmetry of the bipolar structure is slightly different from that of the optical hourglass. Contrary to the optical structure, the emission region of the molecular lines (at least in some of them) and dust shows a well-defined central component of $\sim 2''$ in size. It appears, that most of the molecular mass ($\sim 60\%$) is concentrated in this compact central region (Kamiński et al. 2021).

2.2. Distance

Until recently, CK Vul was assumed to be at a distance of ~ 0.7 kpc. This value was obtained in Hajduk et al. (2013) from an analysis of images and kinematical structure of the nebula probed by the $H\alpha$ and [N II] lines. However, as pointed out in Kamiński et al. (2021), Hajduk et al. (2013) made a mistake in their calculations. Instead of the inclination angle of the nebula of $i = 25^\circ$ (relative to the sky plane), which resulted from fitting their model image to the observations, they took $i = 65^\circ$ (presumably taken as $90^\circ - 25^\circ$) when deriving the distance. If Hajduk et al. (2013) had taken $i = 25^\circ$, they would have obtained a distance of ~ 3.2 kpc (see also Banerjee et al. 2020). Kamiński et al. (2021) showed that the inclination cannot be larger than $\sim 35^\circ$ and consequently the distance cannot be lower than ~ 2.6 kpc. With their measurements of the radial velocity difference between the outermost tips of the optical hourglass nebula, i.e. ~ 1640 km s $^{-1}$, and adopting $i = 25^\circ$, Kamiński et al. (2021) derived a distance of ~ 3.5 kpc.

The above values of the distance rely on the observed radial velocity difference between the northern and southern tips of the nebula (see Fig. 1 in Hajduk et al. 2013) and on the assumption that the line joining the tips has the same inclination as the main body of the hourglass nebula. The latter may not be the case, given the fact that there are several bipolar structures in the inner nebula that are not perfectly aligned with the axis of the large hourglass (Kamiński et al. 2015, 2021; Eyres et al. 2018).

Both, the inclination angle and the distance can be constrained from modelling the shape of the $H\alpha$ line seen through a long slit and shown in Figs. 3 and 4 of Hajduk et al. (2013). We attempted such a determination and used essentially the same model as that in Kamiński et al. (2021). In particular, a linear ("Hubble law"-like) expansion of the nebula was assumed

$$v = v_0 \frac{r}{r_0},$$

where v is the expansion velocity at a radial distance, r , from the center of the nebula. Simulating long-slit observations at the position shown in Fig. 3 of Hajduk et al. (2013), we were able to reproduce the observed shape of $H\alpha$ as displayed in their Fig. 4. The best fit was obtained for $i = 24^\circ$ and $v_0 = 1200$ km s $^{-1}$ at $r_0 = 30''$. Assuming that the nebular expansion started 340 years ago, the obtained value of v_0 (at $r_0 = 30''$) results in a distance of 2.9 kpc. Note that the observed radial velocity difference between the tips implies, in our model, that the inclination of the line joining the tips is $\sim 30^\circ$.

Finally, Kamiński et al. (2021) derived a distance of ~ 3.8 kpc by modelling of the kinematical structure of molecular lobes seen in interferometric ALMA images of the molecular component of the remnant of CK Vul. Henceforth, we adopt a distance

to CK Vul of 3.3 kpc, which is a mean value from the above determinations.

2.3. Kinematics

CK Vul displays a wide range of outflow velocities. The central region expands relatively slowly, with a typical velocity of $\sim 50 \text{ km s}^{-1}$ (Kamiński et al. 2021). This is the reason why this region remains compact compared to the rest of the remnant. The molecular matter in the lobes expands much faster, with a characteristic velocity of $\sim 300 \text{ km s}^{-1}$ (Kamiński et al. 2021). Even faster outflows are observed in the optical hourglass. According to our analysis described in Sect. 2.2, the matter situated $30''$ from the center of the remnant expands at 1200 km s^{-1} , while the maximum outflow velocity of $\sim 1700 \text{ km s}^{-1}$ is attained in the hourglass tips (cf. panel a in Fig. 1). All the values quoted in this section follow quite closely the linear expansion relation, i.e. $v = 1200 \text{ km s}^{-1}(r/30'')$, which is consistent with saying that all the matter observed now in CK Vul was ejected more or less at the same time, that is, during the outbursts observed in 1670–72.

2.4. Luminosities and energetics

Nova 1670 reached its maximum visual brightness at $m_v \simeq 2.6$ on 30 April 1671 (Shara et al. 1985). Adopting a distance of 3.3 kpc and an interstellar extinction with $A_v \simeq 2.8$ (Tylenda et al. 2019), yields an absolute magnitude $M_v \simeq -12.8$. This corresponds to a luminosity of $\sim 1.0 \times 10^7 L_\odot$, if no bolometric correction (BC = 0.0) is assumed. The power of the outburst of CK Vul by far exceeds that attained by the brightest Galactic red nova, V838 Mon ($M_v = -9.8$ and $L \simeq 1.0 \times 10^6 L_\odot$) in its 2002 outburst (Sparks et al. 2008).

The visual light curve of Nova 1670 (Shara et al. 1985) yields an estimate of the total energy emitted by the object as optical radiation of $\sim 3.3 \times 10^{47}$ erg. This is rather a lower limit to the total radiative energy of the nova, as we do not know when the eruption started (the object was already as bright as ~ 3.0 mag, when it was discovered; see Shara et al. 1985). Moreover, as generally red novae show, the object was likely to emit a significant flux in the infrared in late stages of the eruption. The above value can be compared to the kinetic energy of the molecular ejecta of $\sim 2.3 \times 10^{47}$ erg estimated in Kamiński et al. (2021).

At present, CK Vul radiates mainly in the far-IR, with a maximum flux (λF_λ) at 100–200 μm (Evans et al. 2002; Kamiński et al. 2015). Readily, the central object is obscured, and we can only observe the light re-radiated by dust. A combination of the observed integrated flux with a distance of 3.3 kpc results in a luminosity of $\sim 20 L_\odot$. This is a lower limit to the luminosity of the central star, as the observed dust is clearly concentrated in a compact torus or disc (Eyes et al. 2018; Kamiński et al. 2020) and a certain part of the stellar radiation can escape through polar directions without interacting with dust. However, the observed distribution of dust emission suggests that the escaping part cannot be much higher than the observed one (cf. Eyes et al. 2018). We thus put a value of $100 L_\odot$ as a generous upper limit on the luminosity of the central object in CK Vul.

2.5. Elemental abundances and isotopic ratios

Table 1 presents the elemental abundances and the isotopic ratios measured in CK Vul. The elemental abundances were determined by Tylenda et al. (2019) from their spectroscopic optical observations of the brightest nebular region of CK Vul (cf.

Table 1. Elemental abundances and isotopic ratios.

Element	CK Vul	Sun
H	0.49 ± 0.14	0.74
He	0.51 ± 0.14	0.25
C	$(\sim 7 \times 10^{-4})^a$	2.4×10^{-3}
N	$(1.2 \pm 0.4) \times 10^{-3}$	7.0×10^{-4}
O	$(9.5 \pm 3.8) \times 10^{-4}$	5.8×10^{-3}
Ne	$(7.3 \pm 2.5) \times 10^{-4}$	1.3×10^{-3}
S	$(8.9 \pm 1.4) \times 10^{-5}$	3.1×10^{-4}
Ar	$(2.4 \pm 0.6) \times 10^{-5}$	6.7×10^{-5}
$^{12}\text{C}/^{13}\text{C}$	3.8 ± 1.0	90.
$^{14}\text{N}/^{15}\text{N}$	$20. \pm 10.$	440.
$^{16}\text{O}/^{17}\text{O}$	$\geq 180.^b$	2600.
$^{16}\text{O}/^{18}\text{O}$	$36. \pm 14.$	500.
$^{27}\text{Al}/^{26}\text{Al}$	$7. \pm 3.$	∞

Notes. Elemental abundances are given as mass fractions. ^(a) The mass abundance of C is estimated assuming the number ratio of C to O of about 1, as suggested by the molecular composition of the gas. ^(b) Lower limit.

Fig. 2.7 a and b). The abundances given in Table 1 are taken from Table 6 of Tylenda et al. (2019). Note that the abundance of carbon was not directly measured. From their study of the molecular spectrum of CK Vul, Kamiński et al. (2015, 2017) concluded that the C/O number ratio is close to one. This was inferred from the inventory of molecules compared to molecular species observed around stars with known C to O ratio. Thus, the carbon abundance given in Table 1 was calculated from that of oxygen, assuming C/O = 1 (in number of atoms). The isotopic ratios of the CNO elements are taken from Kamiński et al. (2017), who performed an analysis of the rich molecular spectrum of CK Vul observed in the millimeter and submillimeter region. The ratio of aluminum isotopes was measured by Kamiński et al. (2018), who carried out observations and analysis of the emission lines of AlF in the millimeter-wave spectrum of CK Vul. This was the first detection of an astrophysical molecule containing a radioactive isotope (^{26}Al).

The abundance data obtained for CK Vul are compared in Table 1 to solar values from Asplund et al. (2009). Helium and nitrogen are overabundant, while oxygen is clearly underabundant in CK Vul. As a result, the N/O number ratio is equal to ~ 1.4 and is ~ 10 times higher than in the Sun. All this clearly evidences that the observed matter was processed in the CNO cycles of H burning. The heavier elements, which are not affected by the CNO cycles – that is, Ne, S, and Ar – are, on average, by a factor of ~ 2.7 less abundant than in the Sun. Also, the summed up abundance of C, N, and O – which is not affected by the CNO cycles either – is lower by a similar factor, ~ 3.2 . Readily, the progenitor of CK Vul was formed in an environment ~ 3 times less enriched in heavy elements than the Sun ($[\text{Fe}/\text{H}] \simeq -0.5$).

There are observational hints that the element abundances are not uniform across the ejecta of CK Vul. An analysis of emission maps of different molecules in Kamiński et al. (2020) suggests that the central region (cf. Fig. 1) is more oxygen rich than the bipolar lobes, while the latter are most probably nitrogen-rich and have the C/O number ratio close to one. The bright nebular region investigated by Tylenda et al. (2019) overlaps spatially with the northern molecular lobe. The bright and extended optical components A and B defined in Tylenda et al. (2019) and represented in panel c in Fig. 1 are most certainly physically linked

to that lobe. However, the position of the faint and compact component C suggests that it might belong to the central region, instead. Although the abundance analysis of component C is less certain (due to a faint and lower-quality spectrum) than for components A and B, the derived N/O ratio for component C is about four times lower than that obtained for A and B (see Table 5 in Tylanda et al. 2019). Thus, we can conclude that the matter in the lobes is probably more affected by CNO cycles than that in the central region.

Aside to the discussed elements, an optical absorption line of lithium was observed in the outflow of CK Vul against more distant stars (Hajduk et al. 2013). Although, Kamiński et al. (2023) made an attempt to derive the relative Li abundance and obtained $\log N_{\text{Li}}/N_{\text{tot}} + 12 \approx 2.5$ (mass fraction 2×10^{-9}), the results are very uncertain and not particularly constraining for this study. Lithium abundance and its origin are therefore not discussed here in more detail.

2.6. Masses involved in the molecular envelope

Kamiński et al. (2017) determined parameters of the molecular matter in CK Vul from their single-dish submm observations. They derived the size of the CO emission region, $\phi = 9''6$, and the surface CO density, $\Sigma(\text{CO}) = 3.0 \times 10^{17} \text{ cm}^{-2}$. With the adopted distance to CK Vul ($d=3.3 \text{ kpc}$) we obtain the total number of the CO molecules, $N(\text{CO}) = \pi (0.5\phi d)^2 \Sigma(\text{CO}) \approx 5.1 \times 10^{52}$ and the mass of CO of $\sim 2.4 \times 10^{30} \text{ g}$ or $\sim 1.2 \times 10^{-3} M_{\odot}$. With the mass fraction of oxygen, $\sim 1.0 \times 10^{-3}$ (Table 1), as well as assuming C/O ≈ 1 and that most of carbon and oxygen is locked in CO, we estimate that the total mass of the molecular envelope of CK Vul is $\sim 0.7 M_{\odot}$. A similar estimate, $\sim 0.6 M_{\odot}$, has been given by Kamiński et al. (2021) based on interferometric ALMA maps of CK Vul. However, as these authors warn, the total mass can be even higher than $\sim 0.8 M_{\odot}$ when corrected for various observational effects. According to Kamiński et al. (2021), most of the mass ($\sim 60\%$) of the circumstellar matter is concentrated in the central region, while the lobes contain the remaining $\sim 40\%$ of the molecular material.

On the basis of the observed lines of AIF, Kamiński et al. (2018) concluded that the ratio of ^{27}Al to ^{26}Al in CK Vul is ~ 7 and that the observed mass of ^{26}Al is $\sim 7 \times 10^{25} \text{ g}$ ($3.5 \times 10^{-8} M_{\odot}$) (recalculated to a distance of 3.3 kpc). However, the latter value is rather a lower limit on the true amount of ^{26}Al in CK Vul, since the abundance of AIF is limited by the abundance of fluorine rather than that of the much more abundant aluminum.

We estimate the expected total mass of aluminum in the envelope of CK Vul from its presumed abundance. As discussed in Sect. 2.5, heavy elements in CK Vul are underabundant by a factor of ~ 3 compared to the solar composition. We assume that a similar factor holds for aluminum and that the mass fraction of this element is $\sim 1.9 \times 10^{-5}$. Then, we expect $\sim 2.6 \times 10^{28} \text{ g}$ ($1.31 \times 10^{-5} M_{\odot}$) of aluminum in the envelope of CK Vul. If the ratio $^{27}\text{Al}/^{26}\text{Al} \approx 7$ holds for the whole envelope, the total mass of ^{26}Al should be $\sim 3.7 \times 10^{27} \text{ g}$ ($1.85 \times 10^{-6} M_{\odot}$). This should be considered as an upper limit, since the ratio of $^{27}\text{Al}/^{26}\text{Al}$ in outer parts of the envelope is likely to be much higher than the value derived by Kamiński et al. (2018) for the innermost regions.

2.7. Abundance of fluorine

Fluorine is observed in CK Vul only through rotational transitions of the AIF molecule (Kamiński et al. 2017). Detailed ALMA images (Kamiński et al. 2020) show that the emission

of AIF is concentrated in the inner central region of the object. From the surface densities of AIF and CO in the central region, as derived in Kamiński et al. (2020, see their Fig. 8), we can deduce the number ratio $\text{F/O} \approx 2.2 \times 10^{-4}$. Here, we assume that most of the oxygen is locked in CO and most of the fluorine is locked in AIF. The former assumption is probably correct, given that C/O ≈ 1 in the envelope of CK Vul. However, it is questionable whether we observe all the fluorine via AIF lines, as the existence of other molecules bearing this element, for example HF, is not excluded. Thus, the above value of 2.2×10^{-4} is most probably a lower limit to the F/O ratio in CK Vul. Note that the solar value of F/O is 7.4×10^{-5} .

3. Interpretation

In this section, we present an interpretation of the observational results discussed so far in the framework of the hypothesis that the Nova 1670 event resulted from a merger of a binary system. We are going to constrain parameters and the evolutionary status of the stars before the merger, as well as the nature of physical processes that occurred during the merger event. We start with constraining the primary component by identifying the star that was responsible for the principal characteristics of the observed chemical composition of CK Vul.

3.1. The nature of the progenitor primary

The low luminosity of CK Vul, $20 L_{\odot} < L < 100 L_{\odot}$ (see Sect. 2.4), indicates that the central object is not a massive star. Stars more massive than $\sim 3 M_{\odot}$ are more luminous than $100 L_{\odot}$ at any evolutionary stage (Iben 1985; Karakas & Lattanzio 2014). The primary (and the secondary) of the progenitor binary could not have been more massive than that. We can also exclude an AGB star of any mass as the primary (or secondary) of the progenitor. The dense CO-core would have easily survived a merger with almost any other star and the remnant would now be at least as luminous as the progenitor, i.e. $> 10^3 L_{\odot}$.

The observed abundances in CK Vul (overabundance of helium and nitrogen, underabundance of oxygen – see Table 1) evidently show that some part of the observed matter has been processed in the CNO cycles of H burning. This and the presence of ^{26}Al strongly favor the red-giant-branch (RGB) phase of the progenitor primary (if a massive or AGB star is excluded, see above). Moreover, the abundance of ^{26}Al shows that it had to be an evolutionarily advanced RGB star, since the isotope of ^{26}Al is effectively produced in low-mass RGB stars only when the He-core mass is $\geq 0.2 M_{\odot}$.

The only way to obtain ^{26}Al is to activate the MgAl chain, which includes the $^{25}\text{Mg}(p,\gamma)^{26}\text{Al}$ reaction. This takes place when the burning temperature exceeds $3.0 \times 10^7 \text{ K}$ (e.g., Arnould et al. 1999). Then, ^{25}Mg is converted to ^{26}Al in the H-burning shell. ^{26}Al is unstable and decays through $^{26}\text{Al}(\beta^+)^{26}\text{Mg}$ on a (*e*-folding) timescale $\tau_{\beta^+} = 1.03 \times 10^6 \text{ yr}$ (Auer et al. 2009).

We can estimate the luminosity of the presumed RGB star from the observed mass of ^{26}Al . The luminosity of an RGB star, L , is related to the rate of burning hydrogen in the star, $\zeta(\text{H})$, through

$$L = \epsilon_{\text{CNO}} \zeta(\text{H}),$$

where ϵ_{CNO} is energy obtained from burning a unit mass of hydrogen in the CNO cycles ($\epsilon_{\text{CNO}} = 6.0 \times 10^{18} \text{ erg g}^{-1}$).

Let us assume that all ^{25}Mg existing in the unprocessed matter is converted to ^{26}Al in the H-burning shell. The rate of this

process is related to the speed of the hydrogen burning, so we can write

$$\zeta(^{25}\text{Mg}) = \zeta(\text{H}) \frac{X(^{25}\text{Mg})}{X(\text{H})},$$

where $X(^{25}\text{Mg})$ and $X(\text{H})$ are the mass fractions of ^{25}Mg and H, respectively, prior to the H burning. Let us further assume that the distribution of ^{26}Al in the He core is governed by the production of this isotope in the H-burning shell and its subsequent β^+ decay in the core. The rate of production of ^{26}Al , $\xi(^{26}\text{Al})$, is equal to the rate of destruction of ^{25}Mg , $\zeta(^{25}\text{Mg})$. Then the total mass of ^{26}Al in the core, $M(^{26}\text{Al})$, is given by

$$M(^{26}\text{Al}) = \xi(^{26}\text{Al}) \tau_{\beta^+}.$$

After a simple transformation of the above formulae, we get

$$L = \frac{\epsilon_{\text{CNO}}}{\tau_{\beta^+}} \frac{X(\text{H})}{X(^{25}\text{Mg})} M(^{26}\text{Al}).$$

Assuming that the initial abundance of magnesium in the CK Vul progenitor was 3 times lower than that in the Sun and that 10% of it was in the form of ^{25}Mg (like in the Sun – see Asplund et al. 2009), we get $X(\text{H})/X(^{25}\text{Mg}) = 3.0 \times 10^4$. Then the above formula can be rewritten as

$$L = 285 L_{\odot} \frac{M(^{26}\text{Al})}{1.0 \times 10^{-7} M_{\odot}}.$$

Substituting the upper and lower limits on the observed mass of ^{26}Al derived in Sect. 2.6, i.e. $3.5 \times 10^{-8} M_{\odot} < M(^{26}\text{Al}) < 1.85 \times 10^{-6} M_{\odot}$, to the above formula, we obtain limits on the luminosity of the CK Vul progenitor, namely

$$100 L_{\odot} < L < 5300 L_{\odot}.$$

These are fairly consistent with the values expected for low-mass stars in an advanced RGB phase, that is, those having the He-core mass of 0.3–0.45 M_{\odot} and the corresponding luminosity of 100–2000 L_{\odot} (cf. Spada et al. 2017; Hidalgo et al. 2018).

The lack of optical detection of the very highly dust-embedded product of the merger can also be used to infer the properties of the progenitor. MacLeod et al. (2022) considered dust condensation in systems undergoing a merger and found relations between accumulated dusty material and the ‘‘compactness’’ of the primary progenitor, namely between the mass and radius of the progenitor and the circumstellar extinction in the orbital plane, parametrized by A_V . Using their relation, we can constrain A_V in CK Vul. In R -band observations of the field of CK Vul of Hajduk et al. (2013), the weakest detected stars have ~ 22.5 mag. Adopting again the interstellar extinction of $A_R \approx A_V = 2.8$ mag, we take 25.3 mag as a lower limit on the R -band magnitude of the star. Then, to hide any star with a luminosity $> 20 L_{\odot}$ (Sect. 2.4), the dusty torus surrounding CK Vul should cause reddening with $A_V \gtrsim 11$ mag. In this derivation, we considered stellar colors and absolute magnitudes of giants, red supergiants, and main-sequence stars of intermediate spectral types. Reinstating our argument from the beginning of this section, that the progenitor had to be of a mass lower than $\sim 3 M_{\odot}$, we find from MacLeod et al. (2022) that to form a thick torus with $A_V \gtrsim 11$ mag, the primary progenitor had to be large, with a radius consistent – for a given mass – with an RGB phase; for instance, we get a radius $> 40 R_{\odot}$ for a 1 M_{\odot} star.

We conclude that the primary component of the CK Vul progenitor binary was most probably a low-mass (initial mass of ~ 1 – $2 M_{\odot}$) star in the RGB phase.

3.2. Simulation of the observed abundances

The abundances in CK Vul in Table 1 suggest that we observe the dispersed matter that was dredged up from the outer layers of the He core of the RGB primary and that was mixed with the unprocessed matter from the envelope. In order to show that it is very likely the case, we performed simple simulations. Using the Tycho-6.0 (Young et al. 2001; Arnett 2013) and MESA (Modules for Experiments in Stellar Astrophysics; release 21.12.1 Paxton et al. 2011, 2013, 2015, 2018, 2019; Jermyn et al. 2023), we followed the evolution of a 1.0 M_{\odot} star up to the tip of the RGB². Solar abundances (Asplund et al. 2009) were adopted in the initial model, but elements heavier than He were depleted by a factor of 3 in Tycho ([Fe/H] = -0.5); equivalently, $Z=0.008$ was adopted in MESA. We then took the stellar model at the time when its He core had a mass of 0.40 M_{\odot} and mixed the outer 0.1 M_{\odot} region of the He core with the unprocessed envelope material. The mixed abundances were compared to those of CK Vul. We tried to obtain the best fit by changing the fraction of the He-core material in the final mixture, f_{He} . The mass fractions of the elements whose abundances were determined from the observations, that is, H, He, N, O, and Ne (those of S and Ar remain unchanged in the H-burning processes), were taken into account in the fitting procedure in which we searched for the lowest sum of relative squared deviations between the simulated ($X_{n,\text{sim}}$) and observed ($X_{n,\text{obs}}$) abundances, i.e.

$$\chi^2(f_{\text{He}}) = \sum_{n=\text{H, He, O, Ne}} \frac{(X_{n,\text{obs}} - X_{n,\text{sim}})^2}{X_{n,\text{obs}}^2}.$$

The best fit was obtained for $f_{\text{He}}=0.40$ using both Tycho and MESA abundances. The results are compared in Table 2. Except for F which was not considered in the fit, the elemental abundances are fairly consistent between the two evolution packages used.

As can be seen from Table 2, the abundances of the five considered elements are reproduced quite well in our simulations. (To save time, S, Ar, and Al abundances were not considered in MESA.) The relative mixed abundances of the CNO elements and the $^{27}\text{Al}/^{26}\text{Al}$ ratio are also relatively well reproduced, especially by Tycho calculations. This was achieved by adjusting only one parameter. The success of this simple model can be regarded as a strong argument in favor of our hypothesis that the matter observed in CK Vul comes from the He core and the H-rich envelope of an advanced RGB star.

There are, however, inconsistencies between the model results and the observed values. Of first concern are the isotopic ratios of the CNO elements, especially if MESA results are considered because MESA predicts much lower abundances of ^{17}O and ^{18}O than Tycho. Also, the abundances of C, F, and Ne are slightly below the observed values. Clearly, some part of the observed matter had to be also processed in nuclear reactions other than just the equilibrium H burning. We discuss this point further in Sect. 3.4.

3.3. The nature of the progenitor secondary

Within our hypothesis, the required mixing of the matter from the He core with that from the H-rich envelope is caused by the merger of two stars. In other words, the merger event has to disrupt a large portion of the He core. In order for this to happen, the secondary has to have a core that is at least as dense as that of

² The MESA inlist file is available under DOI 10.5281/zenodo.10027069 and <https://doi.org/10.5281/zenodo.10027069>

Table 2. Simulated elemental abundances and isotopic ratios (see text) compared to ones observed in CK Vul.

element	H-envelope	He-core (outer 0.1 M_{\odot})	mixed $f_{\text{He}}=0.40$	CK Vul	mixed $f_{\text{He}}=0.40$	H-envelope	He-core (outer 0.1 M_{\odot})
integrated Tycho mass fraction				observed	integrated MESA mass fraction		
H ^a	0.74	0.00	0.44	0.49	0.43	0.72	0.00
He ^a	0.25	1.00	0.55	0.51	0.56	0.28	1.00
C	7.6×10^{-4}	6.0×10^{-5}	4.8×10^{-4}	$(7 \times 10^{-4})^b$	3.8×10^{-4}	5.9×10^{-4}	5.6×10^{-5}
N ^a	2.2×10^{-4}	2.6×10^{-3}	1.2×10^{-3}	1.2×10^{-3}	1.2×10^{-3}	3.2×10^{-4}	2.6×10^{-3}
O ^a	1.8×10^{-3}	6.1×10^{-5}	1.1×10^{-3}	9.5×10^{-4}	1.1×10^{-3}	1.9×10^{-3}	3.3×10^{-5}
F	1.6×10^{-7}	2.0×10^{-10}	9.5×10^{-8}	$(>2.3 \times 10^{-7})^c$	3.3×10^{-10}	5.6×10^{-10}	3.1×10^{-12}
Ne ^a	4.0×10^{-4}	3.4×10^{-4}	3.8×10^{-4}	7.3×10^{-4}	3.9×10^{-4}	4.2×10^{-4}	3.4×10^{-4}
S	9.8×10^{-5}	9.8×10^{-5}	9.8×10^{-5}	8.9×10^{-5}			
Ar	2.1×10^{-5}	2.1×10^{-5}	2.1×10^{-5}	2.4×10^{-5}			
integrated Tycho number ratio				observed	integrated MESA number ratio		
C/O	0.55	1.28	0.57	$\sim 1^b$	0.86	0.31	1.68
N/O	0.14	48.6	1.19	1.38	31.29	0.17	77.97
F/O	7.4×10^{-5}	2.7×10^{-6}	7.3×10^{-5}	$(>2 \times 10^{-4})^c$	2.2×10^{-7}	3.0×10^{-7}	9.6×10^{-8}
¹² C/ ¹³ C	99.	3.5	48.	3.8	19.8	30.2	4.3
¹⁴ N/ ¹⁵ N	470.	28000.	3700.	20.0	9554.	457.	23200.
¹⁶ O/ ¹⁷ O	2780.	9.6	410.0	$\geq 180.$	1803.	2338.	999.
¹⁶ O/ ¹⁸ O	590.	26000.	600.0	36.0	5.1×10^5	500.	1.3×10^6
²⁷ Al/ ²⁶ Al	∞	2.4	6.0	7.0			

Notes. ^(a) Quantity included in the mixture fit. ^(b) C/O number ratio was assumed (see text). ^(c) A rough lower limit; see Sect. 2.7.

the primary. This rather rules out a main-sequence (MS) star as the secondary. At the base of the layer rich in ²⁶Al, the density of the RGB He core is two orders of magnitude higher than that in the center of lowest-mass MS stars (e.g., Iben 1974). Thus, the He core of an advanced RGB star would survive the merger with a low-mass MS star, remaining practically intact. Consequently, any dredge up of matter from within the He core would be impossible. Moreover, the remnant of such an MS-RGB merger would remain an RGB star with a luminosity of $10^2 - 10^3 L_{\odot}$, which is significantly higher than that of CK Vul.

Instead, a helium white dwarf (HeWD) would meet the observational requirements as the secondary of the binary progenitor of CK Vul. A HeWD can be significantly more compact than an RGB He core of a similar mass (e.g., Hall & Tout 2014). In other words, a He WD can be even several times denser than the RGB core (e.g., Iben 1974). Therefore, in the case of a merger of an RGB star with a HeWD, the He RGB core would become disrupted and finally would form a He-rich envelope around the WD. Since originally the He core was surrounded by a H-rich envelope, it is very likely that the matter from the outer layers of the He core would be mixed with that from the H envelope (for a fuller discussion of the possible scenarios, see Zhang & Jeffery 2013). The merger event releases a lot of energy, therefore some part of the mixed matter would gain enough energy to be dispersed around the system (e.g., Piersanti et al. 2010). After a certain time, it could be observed as a dusty and molecular circumstellar envelope of the remnant. The proposed concepts are schematically illustrated in Fig. 2.

The existence of a HeWD in the progenitor binary indicates that the two stars interacted in the past. It is therefore consistent with the progenitor being a close system prone to instabilities leading to a merger. Independent of that, Kamiński et al. (2021) speculated that the merger binary had a companion which is currently interacting with the merger ejecta. If confirmed, that would make CK Vul progenitor a triple star.

3.4. Nuclear burning during the merger

The merger of an RGB star with a HeWD can also explain the inconsistencies between our modelling and the observations summarized in Table 2, that is, the low values of the observed isotopic ratios of the CNO elements and enhanced abundances of C, F, and Ne.

Let us consider the ¹⁶O/¹⁸O ratio, which is unexpectedly low in CK Vul. The only way to produce a significant amount ¹⁸O is to activate He burning. Then, ¹⁴N, which is the second most abundant isotope after ⁴He in the matter that has been processed in the CNO cycles, is converted to ¹⁸O through ¹⁴N(α, γ)¹⁸F(β^+)¹⁸O. However, at the end of He burning, ¹⁸O is converted to ²²Ne (see Fig. 10 in Arnould et al. 1999). Therefore, an enhanced abundance of ¹⁸O can be taken as evidence of partial He burning (e.g. Clayton et al. 2007).

Helium burning generally requires temperatures above $\sim 1.0 \times 10^8$ K. Mergers of a HeWD with an RGB He core can reach it (Zhang & Jeffery 2013). Objects of this kind and of a mass of 0.3–0.4 M_{\odot} , when approaching each other, attain orbital velocities of ~ 2000 km s⁻¹. Parcels of He-rich matter, when colliding at these velocities, may attain temperatures of up to $\sim 2.0 \times 10^8$ K. Following models of mergers of a HeWD with a CO WD (e.g. Longland et al. 2011; Staff et al. 2012), we can thus expect in our case that after disruption of the RGB He core, a short-lived, hot He-rich layer is formed above the HeWD, whereby partial He burning can occur and ¹⁸O can be effectively produced. Once He burning is activated, we can also expect increased abundances of ¹²C, ¹⁹F and ²²Ne (see e.g. Figs. 10 and 11 in Arnould et al. 1999). This is thus a viable scenario to explain the observed overabundance of C, F, and Ne in Table 2. The case of CK Vul is a strong observational hint that at least some HeWD-RGB mergers activate He burning, despite earlier controversies on the topic (see Piersanti et al. 2010, and references therein).

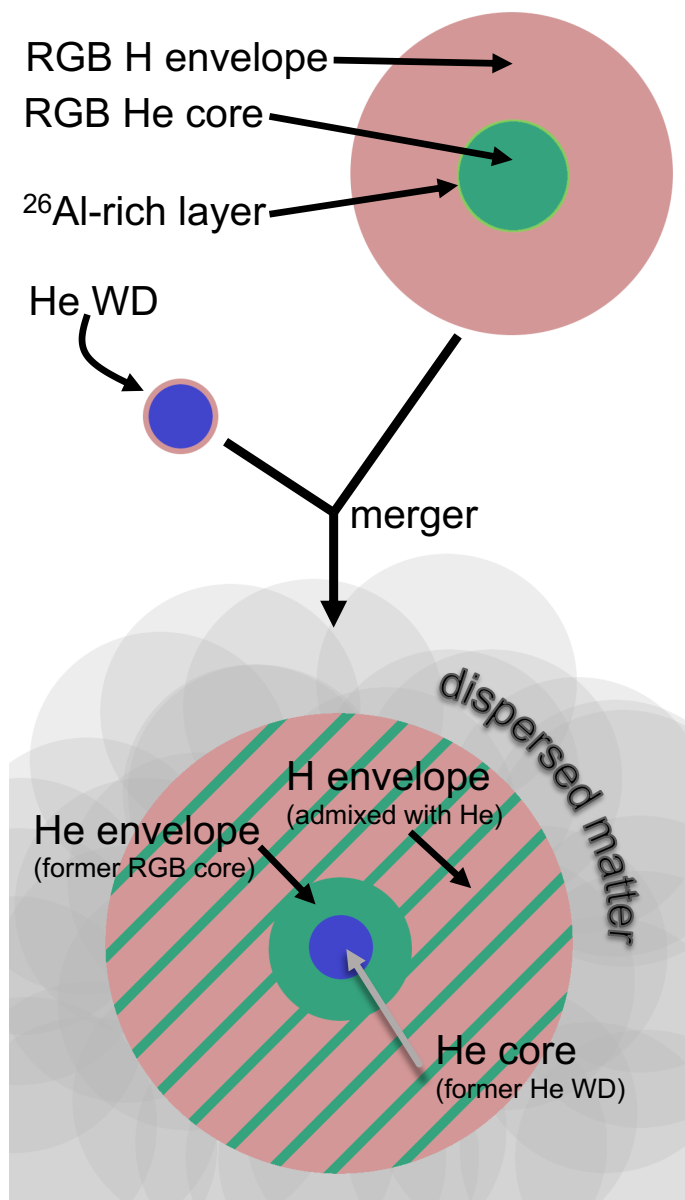


Fig. 2. Schematic illustration of the proposed scenario of a merger between an RGB star with a HeWD, and of its product. The relative sizes of the internal substructures of the stars are not to scale. Pink regions show H-rich matter; dark green represents He-rich gas; light green shows the thin ^{26}Al layer; and blue depicts the He core of the WD.

Stellar mergers are accompanied by strong mixing processes. In this way, matter from stellar interiors can be observed in the outermost regions of the merger product. In our case, it can be also expected that parcels of H-rich gas from the RGB envelope are admixed to the hot He-rich matter. This would activate, perhaps for a short time, initial reactions of the CNO cycles, leading to an enhancement of ^{13}C and, possibly, of ^{17}O in the merger remnant. The enhanced abundance of ^{18}O in the He-rich matter (after having suffered from partial He burning) would also allow production of ^{15}N via $^{18}\text{O}(p,\alpha)^{15}\text{N}$.

3.5. Contribution of He-burning to the energetics

As mentioned in Sect. 2.5, the C/O number ratio is probably close to one in CK Vul, which gives the C mass fraction

$\sim 7 \times 10^{-4}$ (see Table 1). The simple model presented in Sect. 3.2 is not able to meet this figure (see Table 2). However, within our hypothesis of partial He burning, we can get additional carbon. Converting $\sim 4 \times 10^{-4}$ of the observed helium to carbon would be enough to get the desired C abundance. Burning $\sim 1 \times 10^{29}$ g ($5 \times 10^{-4} M_{\odot}$) of helium would output energy of 6×10^{46} erg. This is $\sim 12\%$ of the observed energy released by Nova 1670 (see Sect. 2.4). Only a rather small fraction of this He-burning energy would contribute to the observed radiative luminosity. Most of it would probably be released in various forms of mechanical energy (overcoming the gravitational potential, kinetic energy of the outflowing matter, low- and large-scale turbulent motions, etc.).

3.6. Kinematics of the merger outflow

The merger of an RGB star with a WD explains not only the observed elemental abundances and the isotopic ratios but also the wide range of the observed outflow velocities, i.e. from $\sim 50 \text{ km s}^{-1}$ in the compact equatorial region up to $\sim 1700 \text{ km s}^{-1}$ in the tips of the optical hourglass (see Sect. 2.3 and Fig. 1). At the beginning of the merger, when the WD and the RGB core spiral in the extended common envelope, the matter is lost mainly in the orbital plane with velocities characteristic of winds from red giants, i.e. a few tens of km s^{-1} . This creates a dense equatorial belt of slowly expanding matter. At the final merger, when the WD coalesces with the He-core, the matter is lost with velocities comparable to the escape velocity of a WD, i.e. a few thousand km s^{-1} . This fast outflow is however blocked in the equatorial directions by the dense slow-moving belt of the previously lost matter. In the polar directions, the fast outflow expands relatively freely. In the above scenario, the bipolar lobes should be more enriched in the nuclear ashes than the equatorial belt. This is observed in the remnant of CK Vul, for instance, C/O and N/O are enhanced in the lobes (Sect. 2.5).

3.7. Luminosity of the remnant

At present, 350 years after the merger, the remnant of CK Vul is likely to have a dense He-core (the former HeWD) in its center, surrounded by an extended He-rich layer (the former He-core of the RGB primary) and an outer H-rich envelope (a part of the former H-rich envelope of the primary). The structure is schematically illustrated in Fig. 2. It is easy to show that an object like that should be practically devoid of nuclear power sources. The He core has a too low mass to ignite He in its center. The base of the H-rich envelope, situated above the extended He layer, is most probably insufficiently hot and dense to start H burning. This explains the low current-day luminosity of CK Vul ($< 100 L_{\odot}$).

4. Discussion

In the previous section, we have come to a conclusion that the merger of an RGB giant and a HeWD can consistently account for the main observational data of CK Vul. This scenario allows us to explain and understand the observed elemental abundances, isotopic ratios, kinematics in the nebula, as well as the low luminosity of the object in the contemporary epochs.

Alternatively, however, a merger of two RGB stars could also account for the observational characteristics of CK Vul. The main difference is that in the case of a double RGB merger, ^{26}Al would come from disrupted outer layers of the more massive He core and that a major body of this core would survive the merger

and form a core of the remnant. However, we consider this scenario as less probable than the RGB-HeWD merger, because it would imply almost equal masses of the binary components at the zero-age main sequence (ZAMS). Our Tycho-6 modelling shows that the difference in masses of the components should be $\lesssim 3\%$, in order to satisfy the condition that the less massive star enters the RGB phase before the more massive one leaves it (see also Segev et al. 2019). Although little probable, the case of a double RGB star merger cannot be excluded. All the more that a collision of two RGB stars would probably more likely result in merging of the two cores than merging an RGB core with a HeWD. This is because the common envelope resulting from two RGB envelopes is expected to be more massive than that from a HeWD and a red giant.

It is interesting and instructive to note that our preferred scenario of a merger of a HeWD with an RGB star has been proposed to explain the origin of early-R and J type stars (e.g. Izzard et al. 2007; Zhang & Jeffery 2013; Zhang et al. 2020). These are a special type of carbon stars (Dominy 1984; Abia & Isern 2000; Zamora et al. 2009), with enhanced nitrogen and lithium, a low $^{12}\text{C}/^{13}\text{C}$ ratio, solar O abundances, solar or slightly sub-solar metallicities, and no *s*-element enrichment. Most probably, they are single stars (McClure 1997). The early-R type stars have magnitudes similar to the red-clump stars, which suggests they are in the core He-burning phase. J-type stars are even brighter.

It is tempting to ask whether CK Vul is evolving toward an early R-type star. The answer is not straightforward. In mergers between HeWDs and RGB stars considered by Zhang et al. (2020), simulations show that carbon stars are produced only for high-mass ($\geq 0.45 M_{\odot}$) WDs and at metallicities higher than what we adopted for the CK Vul progenitor. Whether CK Vul remnant is becoming a He-burning carbon star similar to early-R type stars will become more clear when the nebula, especially its dense equatorial waist, disperses and the central star becomes visible. Meanwhile, the low luminosity of CK Vul argues in favor of it becoming an R-type star. Its presumable structure, outlined in Sect. 3.7, is very likely to evolve toward the core He-burning phase. The N overabundance in the nebula is also in favor of that, and so is the low $^{12}\text{C}/^{13}\text{C}$ ratio. The observational indications that C/O ≈ 1 in the molecular lobes and C/O < 1 in the central dense waist may suggest that the star is going to become, or perhaps already is, a carbon star (C/O > 1). As mentioned in Sect. 2.5, lithium appears to be overabundant in the outflow of CK Vul (see also discussion in Kamiński et al. 2023), which is also in line with early-R stars characteristics. The only observational results that make CK Vul appear different from the early R-type stars are the abundances of oxygen and heavier elements. While R-type stars usually show the O abundances and metallicities roughly solar (Dominy 1984; Zamora et al. 2009), in CK Vul oxygen and heavier elements are significantly underabundant. As to oxygen, we may note that observational determination of the O abundance is difficult in carbon stars. It is often estimated from scaling with the metallicity (e.g. Zamora et al. 2009). Nevertheless, in a sample of five early R-type stars, for which Dominy (1984) were able to reliably estimate the O abundance, there is one star, HD 100764, with both parameters close to those found for CK Vul, i.e. [O] ≈ -0.53 and [Fe] ≈ -0.59 (versus [O] ≈ -0.60 and [Fe] ≈ -0.31 in CK Vul).

In conclusion, it is very likely that the historical Nova 1670 resulted from a merger of a HeWD and an RGB star, and that its remnant, CK Vul, is now evolving toward becoming an early R-type star.

Acknowledgements. TK acknowledges funding from grant SONATA BIS no 2018/30/E/ST9/00398 from the Polish National Science Center. RS acknowl-

edges support from the Polish National Science Center grant SONATA BIS 2018/30/E/ST9/00598

References

- Auer, M., Wagenbach, D., Wild, E. M., et al. 2009, *Earth and Planetary Science Letters*, 287, 453
- Abia, C. & Isern, J. 2000, *ApJ*, 536, 438
- Arnett, D. 2013, *Astrophysics Source Code Library*. ascl:1303.008
- Arnould, M., Goriely, S., & Jorissen, A. 1999, *A&A*, 347, 572
- Asplund, M., Grevesse, N., Sauval, A. J., & Scott, P. 2009, *ARA&A*, 47, 481
- Banerjee, D. P. K., Geballe, T. R., Evans, A. et al. 2020, *ApJ*, 904, L23
- Blöcker, T. 1995, *A&A*, 299, 755
- Clayton G. C., Geballe T. R., Herwig F., et al. 2007, *ApJ*, 662, 1220
- Crause, L. A., Lawson, W. A., Kilkenny, D., et al. 2003, *MNRAS*, 341, 785
- De Marco, O., Passy, J. C., Moe, M., et al. 2011, *MNRAS*, 411, 2277
- Dominy, J. F. 1984, *ApJS*, 55, 27
- Evans, A., van Loon, J. Th., Zijlstra, A. A., et al. 2002, *MNRAS*, 332, L35
- Eyres, S. P. S., Evans, A., Zijlstra, A., et al. 2018, *MNRAS*, 481, 4931
- Hajduk, M., Zijlstra, A. A., van Hoof, P. A. M., et al. 2007, *MNRAS*, 378, 1298
- Hajduk, M., van Hoof, P. A. M., & Zijlstra, A. A. 2013, *MNRAS*, 432, 167
- Hall, P. D. & Tout, C. A. 2014, *MNRAS*, 444, 3209
- Hidalgo, S. L., Pietrinferni, A., Cassisi, S., et al. 2018, *ApJ*, 856, 125
- Harrison, T. E., 1996, *PASP*, 108, 1112
- Iben, I. 1974, *ARA&A*, 12, 215
- Iben, I. 1985, *QJRAS*, 26, 1
- Izzard R. G., Jeffery C. S., & Lattanzio J., 2007, *A&A*, 470, 661
- Jermyn, A. S., Bauer, E. B., Schwab, J., et al. 2023, *ApJS*, 265, 15
- Kamiński, T., Mazurek, H. J., Menten, K. M., et al. 2022, *A&A*, 659, A109
- Kamiński, T., Menten, K. M., Tylenda, R., et al. 2015, *Nature*, 520, 322
- Kamiński, T., Menten, K. M., Tylenda, R., et al. 2017, *A&A*, 607, A78
- Kamiński, T., Tylenda, R., Menten, K. M., et al. 2018, *Nature Astronomy*, 2, 778
- Kamiński, T., Schmidt, M., Hajduk, M., et al. 2023, *A&A*, 672, A196
- Kamiński, T., Steffen, W., Tylenda, R. et al. 2018, *A&A*, 617, A129
- Kamiński, T., Menten, K. M., Tylenda, R. et al. 2020, *A&A*, 644, A59
- Kamiński, T., Steffen, W., Bujarrabal, V. et al. 2021, *A&A*, 646, A1
- Karakas, A. I. & Lattanzio, J. C. 2014, *PASA*, 31, e030.
- Kato, T., 2003, *A&A*, 399, 695
- Kimeswenger, S., Lederle, C., Schmeja, S., & Armsdorfer, B. 2002, *MNRAS*, 336, L43
- Longland, R.; Lorén-Aguilar, P.; José, J. et al. 2011, *ApJ*, 737, L34
- MacLeod, M., De, K., & Loeb, A. 2022, *ApJ*, 937, 96
- McClure, R. D. 1997, *PASP*, 109, 256
- Miller Bertolami, M. M. 2016, *A&A*, 588, A25.
- Munari, U., Henden, A., Kiyota, S. et al. 2002, *A&A*, 389, L51
- Naylor, T., Charles, P. A., Mukai, K., & Evans, A. 1992, *MNRAS*, 258, 449
- Nelemans, G., Verbunt, F., Yungelson, L. R., & Protegias Zwart, S. F. 2000, *A&A*, 360, 1011
- Paxton, B., Bildsten, L., Dotter, A., et al. 2011, *ApJS*, 192, 3
- Paxton, B., Cantiello, M., Arras, P., et al. 2013, *ApJS*, 208, 4
- Paxton, B., Marchant, P., Schwab, J., et al. 2015, *ApJS*, 220, 15
- Paxton, B., Schwab, J., Bauer, E. B., et al. 2018, *ApJS*, 234, 34
- Paxton, B., Smolec, R., Schwab, J., et al. 2019, *ApJS*, 243, 10
- Piersanti, L., Cabezón, R. M., Zamora, O., et al. 2010, *A&A*, 522, A80
- Segev, R., Sabach, E., & Soker, N. 2019, *ApJ*, 884, 58
- Shara, M. M., Moffat, A. F. J., & Webbink, R.F. 1985, *ApJ*, 294, 271
- Soker, N. & Tylenda, R. 2003, *ApJ*, 582, L105
- Spada, F., Demarque, P., Kim, Y.-C., et al. 2017, *ApJ*, 838, 161
- Sparks, W. B., Bond, H. E., Cracraft, M., et al. 2008, *AJ*, 135, 605
- Staff, J. E.; Menon, A.; Herwig, F. et al. 2012, *ApJ*, 757, 76
- Tylenda, R. & Soker, N. 2006, *A&A*, 451, 223
- Tylenda, R., Hajduk, M., Kamiński, T. et al. 2011, *A&A*, 528, A114
- Tylenda, R., Kamiński, T., Udalski, A. et al. 2013, *A&A*, 555, A16
- Tylenda, R., Kamiński, T., & Mehner, A., 2019, *A&A*, 628, A124
- Young, P. A., Mamajek, E. E., Arnett, D., & Liebert, J. 2001, *ApJ*, 556, 230
- Zamora, O., Abia, c., Plez, B. et al. 2009, *A&A*, 508, 909
- Zhang, X., & Jeffery, C. S., 2013, *MNRAS*, 430, 2113
- Zhang, X., Jeffery, C. S., Li, Y., & Bi, S., 2020, *ApJ*, 889, 33